# Discrete dislocation plasticity

van der Giessen, E.

*Published in:*
EPRINTS-BOOK-TITLE



*Publication date:*
2003

# Discrete dislocation plasticity

Erik Van der Giessen

The Netherlands Institute for Metals Research/

Dept. of Applied Physics, University of Groningen, Nyenborgh 4, 9747 AG Groningen, The Netherlands

## 1 Introduction

My overview paper entitled “Plasticity in the 21st century” for the 2000 International Congress on Theoretical and Applied Mechanics [1] had L. Kronecker’s famous expression “God created the integers, all else is the work of man” as a slightly provocative motto. What I wanted to stress with this is that people (like me) who have had a classical mechanics training and whose default thinking about plasticity is in terms of continuum constitutive modeling, there is much to learn by careful rethinking of the discrete nature of the physical vehicles for plastic flow, i.e. dislocations. It seems to me that the subject of “discrete dislocation plasticity” has re-gained momentum during the last decade and has shown interesting potential in an era of continued miniaturization. This article is partly a reinforcement and partly an extension of my 2000 plea for the subject.

With reference to the schematic of pertinent length scales in plasticity in Fig. 1, I will start by pointing out that there is a seemingly growing class of plasticity problems where the relevant length scale (determined either by geometry or by the wavelength of the deformation pattern) is such that there are too few dislocations in order that a continuum plasticity description is meaningful, but at the same time there are too many dislocations for atomistic modeling to be practical. This class of problems is in the realm of discrete dislocation plasticity, in which dislocations are treated as line singularities in an elastic continuum. The solution of discrete dislocation plasticity problems involves two essential ingredients: (i) the determination of the fields inside a dislocated body; (ii) the evolution of the dislocation structure on the basis of the current fields. The basic idea of the approach goes back a long time, and seminal work on the first aspect can be found in the famous textbook by Hirth and Lothe [2]. The drawback in this classical view is that for each boundary value problem the solution of the elasticity problem with a number of dislocations in the studied geometry subject to its boundary conditions needs to be found. Because of the singularity along the dislocation line this is a horrifying task, and in fact only a finite number of relatively simple cases have been solved. In 1995, Alan Needleman and I [3], devised a more versatile approach in which we use the singular part of a known solution (e.g. in infinite space) and employ superposition to augment it with a finite element solution to comply with the actual boundary conditions.

In this paper, the essentials of this approach will be summarized, including the additional ingredients, so-called constitutive rules, needed to analyze dislocation dynamics (limiting attention to two-dimensional situations). The subsequent section will discuss what we have learned

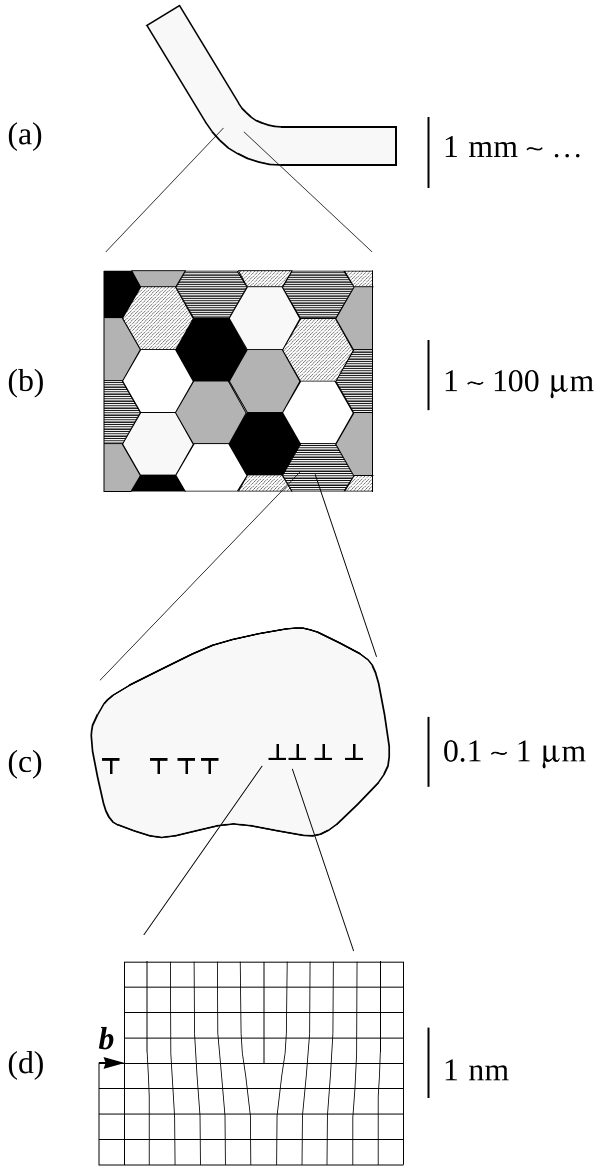


Figure 1: Schematic of the various pertinent length scales in between a single dislocation and a plastically deforming polycrystalline metal at the macro-scale. Each length scale requires its own type of model: (a) macroscopic phenomenological; (b) crystal plasticity; (c) discrete dislocation plasticity; (d) atomistics.

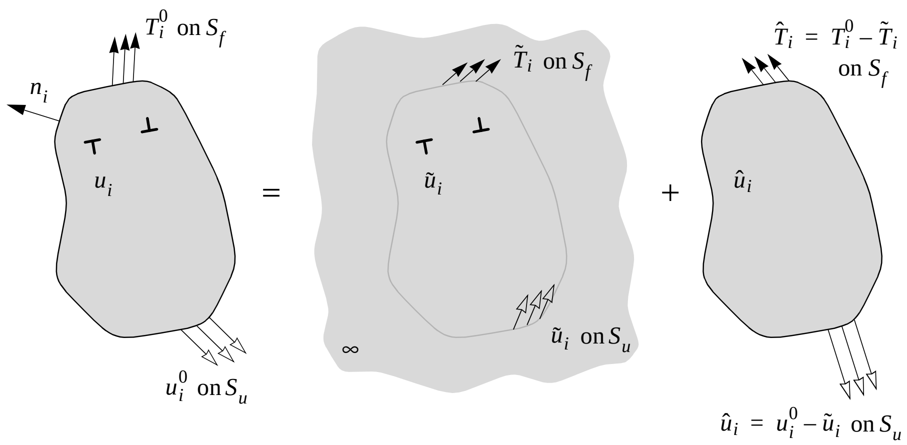


Figure 2: Decomposition into the problem of interacting dislocations in the infinite solid (˜ fields) and the complementary problem for the finite body without dislocations (ˆ or image fields).

from discrete dislocation plasticity in relation to fracture problems under monotonic or fatigue loading. A very important characteristic of discrete dislocation plasticity is that it is inherently size dependent, contrary to classical continuum models. The subsequent section will therefore discuss a number of model problems that we have considered in helping the development of nonlocal continuum plasticity theories by comparing the discrete dislocation results with the solutions of a few recent nonlocal theories.

## 1.1 General approach

In discrete dislocation plasticity, a dislocation is treated as a line singularity in a linear elastic continuum, whose motion produces what we observe as permanent, plastic strain. Such a description obviously cannot capture the core structure of a dislocation, but it does capture the fields further away than five to ten times the atomic spacing. Within the linear elastic approximation, the fields around a dislocation have the typical structure that (i) the displacement component parallel to the slip plane on which it lives is discontinuous across the slip plane and that (ii) the stress and strain fields decay as $1/r$ away from the dislocation. Because of this $1/r$ decay, dislocations have long-range effects and interactions with other dislocations. In addition, these interactions depend in a rather complex manner on the orientation relative to the other dislocations. Owing to these characteristics, dislocations can organize in dislocation structures, such as walls and cells.

For the determination of the fields in an arbitrary dislocated body subject to boundary conditions, the basic idea put forward in [3] was to exploit the known singular solutions, notably in infinite space, and to use superposition to correct for the proper boundary conditions, as illustrated in Fig. 2. The displacement, strain and stress fields are decomposed as

$$u_i = \tilde{u}_i + \hat{u}_i\,, \quad \varepsilon_{ij} = \tilde{\varepsilon}_{ij} + \hat{\varepsilon}_{ij}\,, \quad \sigma_{ij} = \tilde{\sigma}_{ij} + \hat{\sigma}_{ij}\,. \tag{1}$$

The (˜) fields are the superposition of the singular fields of the individual dislocations in their current configuration, but in infinite space. Identifying the fields for dislocation $k$ by a superscript $(k)$, the $(\tilde{\ })$ stress field, for example, is obtained as $\tilde{\sigma}_{ij} = \sum_k \sigma_{ij}^{(k)}$. The actual boundary conditions, in terms of prescribed displacements $u_i^0$ or tractions $T_i^0 = \sigma_{ij} n_j$, are imposed through the $(\hat{\ })$ fields, in such a way that the sum of the $(\tilde{\ })$ and the $(\hat{\ })$ fields in (1) gives the solution that satisfies all boundary conditions. It is important to note that the solution of the $(\hat{\ })$ problem does not involve any dislocations. Therefore, the $(\hat{\ })$ fields (often called 'image' fields) are smooth and the boundary value problem for them can conveniently be solved using a finite element method.

# 2 Constitutive rules

Once the fields in the dislocated solid are known, the second ingredient is to determine the instantaneous change of the dislocation structure. Materials scientists have discovered a variety of different ways in which this may happen, such as (i) (predominantly) dislocation glide; (ii) climb; (iii) cross slip; (iv) annihilation; (v) junction formation with other dislocations and (v) pinning at obstacles. Each of these mechanisms is controlled by atomistic processes, which, by definition, are not resolved in discrete dislocation plasticity. These have to be incorporated by a set of constitutive equations or rules, just like in plasticity theories at higher size scales (Fig. 1a, b). These constitutive rules have to be inferred from experiments or from atomistic simulations.

The important point to note first is that the key quantity involved in constitutive rules for dislocation evolution is the so-called Peach-Koehler force. It is a configurational force acting on the dislocation (per unit length) that is work-conjugate to motions of this dislocation that leave the total length of the dislocation unchanged. It can be shown [3] that in the approach outlined above, the component of the Peach-Koehler force in the slip plane can be expressed as

$$f^{(k)} = n_i^{(k)} \left( \hat{\sigma}_{ij} + \sum_{l \neq k} \sigma_{ij}^{(l)} \right) b_j^{(k)} . \tag{2}$$

This expression highlights the long-range contribution of all other dislocations, through the second term in parentheses, as well as the image stresses.

It would take too far to discuss the constitutive rules in general; we will confine ourselves here to those used in the two-dimensional simulations to be presented later. All these problems involve only edge dislocations, for which the glide component of the Peach-Koehler force reduces to $f^{(k)} = \tau^{(k)} b^{(k)}$ where $\tau^{(k)}$ is the resolved shear stress on the plane. The following ingredients to the evolution of the dislocation structure are incorporated: the motion of dislocations along their slip plane, pinning of dislocations at obstacles, annihilation of opposite dislocations, and generation of new dislocation pairs from discrete sources.

Glide of a dislocation is accompanied by drag forces due to interactions with electrons and phonons. The simplest models of this lead to drag forces that can be expressed as $Bv^{(k)}$ where $B$ is the drag coefficient. A value of $B = 10^{-4}\,\mathrm{Pa\,s}$ is representative for aluminum [4]. When inertia effects of dislocations are ignored, the magnitude of the glide velocity $v^{(k)}$ of dislocation $k$ becomes linearly related to the Peach-Koehler force through $f^{(k)} = Bv^{(k)}$.

New dislocation pairs are generated by simulating Frank-Read sources. The initial dislocation segment of a Frank-Read source bows out until it produces a new dislocation loop and a replica of itself. The Frank-Read source is characterized by a critical value of the Peach-Koehler force, the time it takes to generate a loop and the size of the generated loop. In two dimensions, this is simulated by point sources which generate a dislocation dipole when the magnitude of the Peach-Koehler force at the source exceeds a critical value $\tau_{\rm nuc} b$ during a period of time $t_{\rm nuc}$. The distance $L_{\rm nuc}$ between the dislocations is specified so that the dipole does not collapse onto itself under an applied force of $\tau_{\rm nuc} b$. In the examples shown later, the strength of the dislocation sources is chosen at random from a Gaussian distribution with mean strength $\bar{\tau}_{\rm nuc}$ and standard deviation of $0.2\bar{\tau}_{\rm nuc}$. The nucleation time for all sources is typically taken as $t_{\rm nuc} = 0.01\ \mu$s.

Annihilation of two dislocations with opposite Burgers vector occurs when they are sufficiently close together. This is modeled by eliminating two dislocations when they are within a material-dependent, critical annihilation distance $L_{\rm e}$, which is taken as $L_{\rm e} = 6b$ [4] in the examples later.

In some calculations, obstacles to dislocation motion are included that are modeled as fixed points on a slip plane. Such obstacles can represent either small precipitates or forest dislocations. Pinned dislocations can only pass the obstacles when their Peach-Koehler force exceeds an obstacle dependent value $\tau_{\rm obs} b$.

# 3 Applications to crack problems

Plastic deformation near crack tips can be considered at different length scales. Under the assumption of small-scale yielding, continuum plasticity representations of near-tip fields were established on the basis of isotropic models halfway the last century, and more recently for anisotropic crystal plasticity by Rice [5]. When strain hardening is neglected, the latter fields are predicted to have a remarkable geometry, with the stress state being uniform in distinct sectors around the tip, and with either slip bands or kink bands in between the sectors. Evidently, this analysis ignores the discreteness of dislocations inside the plastic zone.

Cleveringa *et al.* [6] carried out a discrete dislocation analysis of a mode I crack. Crack propagation was modeled by a cohesive surface with fracture properties approaching atomic (de)bonding. Depending on the densities and strengths of the sources and obstacles that were randomly introduced around the crack tip, these calculations showed that (i) crack growth was brittle if insufficient dislocation activity was triggered; (ii) crack blunting without fracture occurred when dislocations could move sufficiently far away from the top to effectively shield the tip; and (iii) in intermediate situations, the crack could grow in spurts due to the fact that dislocation structures formed near the tip that raised the local opening stress state to the cohesive strength over a sufficiently large region. This is demonstrated for a particular case with two slip systems at $\pm 60^\circ$ from the crack plane in Fig. 3. The salient feature of the findings in [6] is that dislocations can play a dual role: On the one hand they are the carriers of plastic relaxation, while at the same time they move with them a singularity.

The other observation made in [6] was that from some distance ($\approx 0.5\mu$m) away from the tip, the stresses appear to be uniform on average in three sectors around the tip, consistent with Rice's [5] continuum crystal plasticity analysis for this orientation of two slip systems. This connection was studied in more detail in [7] for crystals with three slip systems. One of the orientations studied was so that in addition to the two $\pm 60^\circ$ slip systems considered in Fig. 3 there was a slip system with its slip planes parallel to the crack plane. In this case, Rice's analysis predicts four fully plastic, uniform stress sectors in the absence of hardening, with kink

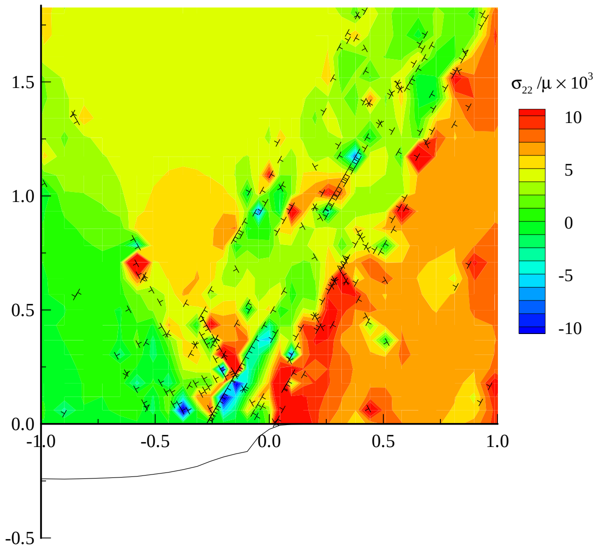


Figure 3: Distribution of dislocations and the opening stress $\sigma_{22}$ in the immediate neighborhood ($2\mu$m $\times$ $2\mu$m) of the crack tip for the case with $\rho_{nuc} = 49/\mu m^2$ ($\bar{\tau}_{nuc} = 50$ MPa) and $\rho_{obs} = 98/\mu m^2$ ($\tau_{obs}$) at the onset of crack growth. The corresponding crack opening profiles (displacements magnified by a factor of 10) are plotted below the $x_1$-axis. From [6].

bands rather than slip bands in between two of these. The average stresses from the discrete dislocation analysis were found to agree fairly well with the continuum predictions, but no sign of kink bands was found. However, the non-hardening continuum slip solutions are not unique and Drugan [8] has constructed alternative elastic-ideally plastic solutions in which kink bands do not form. In fact, there are several solution families without kink bands. For the same configuration analyzed by discrete dislocation plasticity, one of his solution families has a slip band at $\theta = 60°$, consistent with our discrete dislocation simulations. Within this family, the solution that seemed to agree best with the discrete dislocation results, had one of the sectors being elastic (instead of fully plastic) and collapsing to a line discontinuity.

The duality in the role of near-tip dislocations mentioned above is not restricted to the mode I crack problem, but is probably generic for many fracture issues. For example, Deshpande et al. [9] have considered the growth of a crack along the interface with a rigid material under cyclic remote mode I loading, where the near-tip enhanced stress state was again found to determine when the crack would advance. Another discrete dislocation effect that is critical in fatigue is the irreversibility of dislocation motion. A summary of some salient results in [9] shown in Fig. 4, demonstrates that the cyclic crack growth rate $\log(da/dN)$ versus applied stress intensity factor range $\log(\Delta K_I)$ curve that emerges naturally from the discrete dislocation solution shows distinct threshold and Paris law regimes. It is emphasized that no special features were introduced in the discrete dislocation plasticity analysis for fatigue loading. However, the cohesive law used in this calculation was modified to be irreversible, in a simple attempt to account for an oxidizing environment.

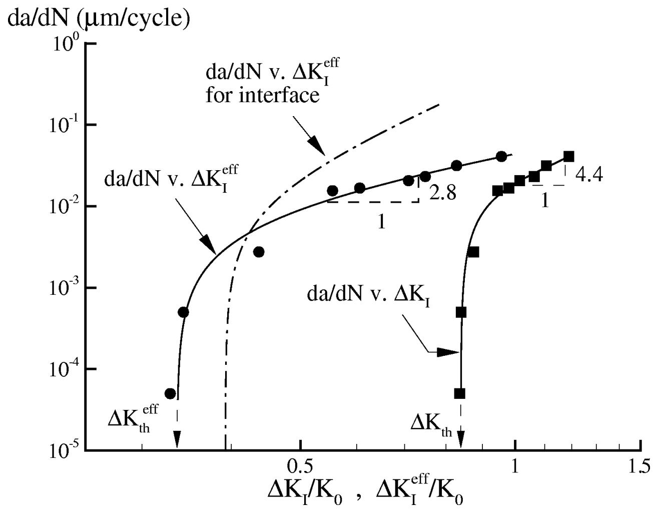


Figure 4: The cyclic crack growth rate $da/dN$ versus $\Delta K_{\mathrm{I}}/K_0$ for the mode I cyclic loading of a single crystal and for an interface crack. The same data is also plotted versus the effective loading amplitude $\Delta K_{\mathrm{I}}^{\mathrm{eff}}$ which accounts for crack closure in the assumed irreversible cohesive surface. The slopes of the curves marked correspond to the Paris law exponents for the curves fitted through the numerical results. From [9].

# 4 On the scale transition to strain gradient continuum theories

With reference to the scale transitions illustrated in Fig. 1, a discrete dislocation description should be able to provide a true foundation for crystal plasticity. The continuum description of plastic deformation in the latter implies an averaging of the behavior of a sufficiently large ensemble of dislocations. Statistical approaches are now starting to be developed, but the link between the two descriptions of plasticity is currently done indirectly through constitutive rules. One of the most important constitutive laws in a crystal plasticity theory is that for hardening of slip systems. From the point of view of discrete dislocations, hardening is largely due to the interactions between the dislocations on the slip system under consideration with those on intersecting slip systems. Three-dimensional discrete dislocation models are capable of simulating this forest hardening mechanism and thereby to provide input to the hardening laws in crystal plasticity models (see, e.g., [10]).

Such simulations, however, deliberately ignore other interactions and are therefore relevant for the behavior in the interior of a grain. The interaction with boundaries, such as interfaces with second-phase particles and grain boundaries gives rise to additional effects. Cleveringa *et al.* [11], for example, performed a discrete dislocation analysis of plastic flow in a model composite material containing hard elastic particles, under single slip conditions. They demonstrated that, depending on the particle shape and size, the material may develop geometrically necessary dislocations. In such cases, the overall response was also found to be dependent on the size of the reinforcements (at the same volume fraction). The corresponding deformation field, shown in Fig. 5a, reveals rotation of the central particle as well as localized shearing near the ends of the particles.

Since the predicted dislocation densities, even for overall strains as small as 1%, reach

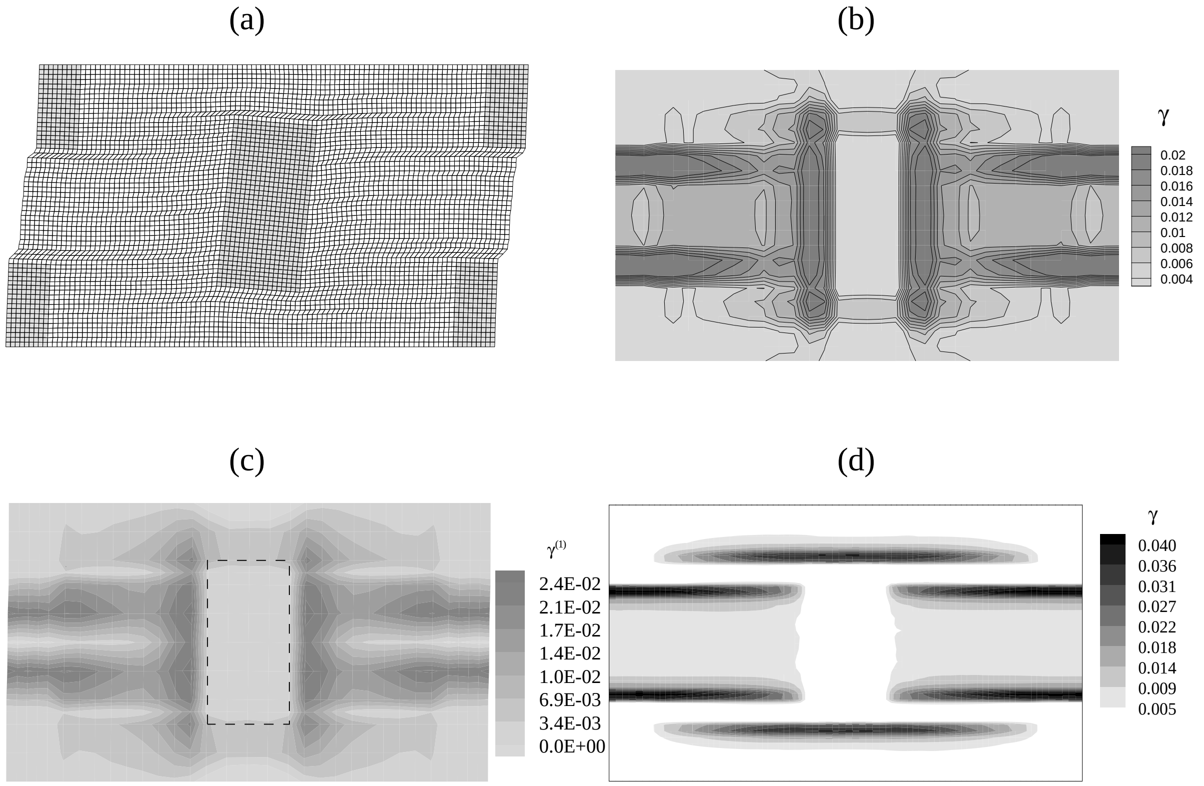


Figure 5: Deformation fields for the composite under simple shear (see inset) according to various theories: (a) deformed mesh (amplified) according to discrete dislocation plasticity (from [11]); (b) slip distribution according to the Acharya-Bassani theory (from [16]); (c) idem according to Gurtin's nonlocal theory [17] and (d) idem according to Groma's theory [15].

values on the order of $10^{14}\mathrm{m}^{-2}$, one may ask the question if the problem could have been analyzed by continuum plasticity. Although standard continuum plasticity theories do predict additional hardening due to the particles [11], they cannot predict size-dependent behavior. For this, one needs nonlocal or strain gradient theories.

There are a number of strain gradient crystal plasticity models available in the literature at the moment. We have analyzed the same problem with three of these: (i) by Acharya and Bassani [16]; (ii) by Gurtin [13]; (iii) by Yefimov *et al.* [14, 15]. These theories differ in several ways. The Acharya–Bassani theory is the simplest one with the strain gradient only entering as an additional contribution to the hardening of a slip system. The Gurtin theory incorporates this effect, but in addition includes kinematic hardening; the latter involves an internal variable that is governed by a separate differential equation with associated boundary conditions. While these mentioned theories are entirely phenomenological, the third theory considered is based on a statistical description of an ensemble of interacting edge dislocations on parallel glide planes by Groma [14]. This leads to two dislocation density fields: one being the total dislocation density, the other being the dislocation-difference density (directly related to the density of geometrically necessary dislocations). These two fields are governed by two coupled transport equations with associated boundary conditions. Making use of the Orowan relationship, Yefimov *et al.* [15] coupled this to a continuum slip theory.

First it should be pointed out that all three nonlocal theories are capable of picking up the size dependence found in the discrete dislocation simulations, by appropriate selection of the material parameters (notably, the length scale parameters entering in the Acharya–Bassani [16] and Gurtin theories [17]). The aspect of the overall response that the Acharya–Bassani theory did not capture was the strong Bauschinger effect seen in [18], because this theory only involves slip system hardening and no kinematic hardening contribution as in the Gurtin theory. The current Groma theory only has kinematic hardening. The deformation fields predicted by these nonlocal theories are also shown in Fig. 5. The Acharya–Bassani prediction, in Fig. 5b, still resembles the local solution [11, 16] but it somewhat smoother and has increased slip above and below the central particle. The slip distribution according to Gurtin's theory, in Fig. 5c, differs from it by the slip on the left and right hand sides of the particle rapidly dropping to zero at the interface, because of the boundary condition imposed their. It seems that Groma's theory predicts a deformation field that is closest to the discrete dislocation result, Fig. 5d vs Fig. 5a, with deformation concentrating into slip bands near the top and bottom of all particles and no slip on the particle sides.

The second example to be briefly discussed here is that of the simple shear of single crystal between rigid walls. Assuming the crystal to have two slip systems with slip planes at $\pm 60^\circ$ from the shearing direction, discrete dislocation simulations predict the development of boundary layers because of the constraint on slip imposed by the impenetrable boundaries. The development of these boundary layers is accompanied by the development of geometrically necessary dislocations, which again induces a size effect [19] Standard continuum theories not only fail to pick up the boundary layers, they also do not capture the size effects. In fact, nonlocal theories that do not have additional (higher-order) boundary conditions also are not able to pick up these effects, because deformation will remain uniform when starting from a homogeneous state, just like in a local theory. The Shu-Fleck [20] and the Gurtin theory [17] both do capture the boundary layer formation and the size effect.

# 5 Concluding remarks

Discrete dislocation plasticity applies to problems that are neither amenable to atomistics nor to continuum theories of plasticity. From this position, it holds promises in two directions.

One is the vertical direction in the length scale picture in Fig. 1: DDP can help to bridge the gap between atomistic descriptions of dislocations and continuum descriptions of crystal plasticity. An obvious route is to fine-tune DDP models on the basis of atomistic studies and to use DDP simulations to provide quantitative input for phenomenological constitutive rules in crystal plasticity. This assumes the existence of a theory. However, the form of crystal plasticity theories that account for size effects is not known; several attempts are being made, but this subject leaves many challenges for the future.

The second direction in which DDP is expected to become a major player is the horizontal direction in Fig. 1, i.e. as a tool to analyze plasticity problems at the micron scale. With the continued miniaturization of components that is expected in this new century, this may become a major application area for DDP. Quantitative predictions, evidently, require a three-dimensional implementation and this is well-underway now (e.g. [4, 21], but there are still a number of technical difficulties to be solved there [22].

# References

[1] Van der Giessen, E. (2001) in *Mechanics for a New Millennium*, ed. by H. Aref and J.W. Phillips. Kluwer Acad. Publ., Dordrecht, pp. 413–428.

[2] Hirth, J.P. and Lothe, J. (1968) *Theory of Dislocations*, McGraw-Hill, New York.

[3] Van der Giessen, E. and Needleman, A. (1995) *Model. Simul. Mater. Sci. Eng.* **3**, 689–735.

[4] Kubin, L.P., Canova, G., Condat, M., Devincre, E., Pontikis, V. and Brechet, Y. (1992) In *Nonlinear Phenomena in Materials Science* II, eds. G. Martin and L.P. Kubin, p. 455., Sci-Tech, Vaduz.

[5] Rice, J.R. (1987) *Mech. Mater.* **6**, 317–335.

[6] Cleveringa, H.H.M., Van der Giessen, E. and Needleman, A. (2000) *J. Mech. Phys. Solids* **48**, 1133–1157.

[7] Van der Giessen, E., Deshpande, V.S., Cleveringa, H.H.M. and Needleman, A. (2001) *J. Mech. Phys. Solids* **49**, 2133–2153.

[8] Drugan, W.J. (2001) *J. Mech. Phys. Solids* **49**, 2155–2176.

[9] Deshpande, V.S., Needleman, A. and Van der Giessen, E. (2002) *Acta Mat.* **50** 831–846.

[10] Fivel, M., Tabourot, L., Rauch, E. and Canova, G. (1998) *J. Phys. IV France* **8** 151–158.

[11] Cleveringa, H.H.M., Van der Giessen, E. and Needleman, A. (1997) *Acta Mater.* **45** 3163–3179.

[12] Acharya, A. and Bassani, J.L. (2000) *J. Mech. Phys. Solids* **48** 1565–1595.

[13] Gurtin, M.E. (2002) *J. Mech. Phys. Solids* **50** 5–32.

[14] Groma, I. (1997) *Phys. Rev. B* **56** 5807–5813.

[15] Yefimov, S., Groma, I. and Van der Giessen, E. (2001) *J. Phys. IV* **11** Pr5/103–110.

[16] Bassani, J.L., Needleman, A. and Van der Giessen, E. (2001) *Int. J. Solids Struct.* **38** 833–853.

[17] Bittencourt, E., Needleman, A., Gurtin, M.E., Van der Giessen E. (2002) *J. Mech. Phys. Solids* (in print).

[18] Cleveringa, H.H.M., Van der Giessen, E. and Needleman, A. (1999) *Phil. Mag.* **A79** 893–920.

[19] Shu J.Y., Fleck N.A. (1999) *J. Mech. Phys. Solids* **47** 297–324.

[20] Shu JY, Fleck NA, Van der Giessen E, Needleman A. *J. Mech. Phys. Solids* **49** 1361-1395.

[21] Weygand, D.M., Friedman, L.H. and Van der Giessen, E. (2001) *Mat. Sci. Engrg.* **A309-310** 420–424.

[22] Weygand, D.M., Friedman, L.H. and Van der Giessen, E. (2001) *Model. Simul. Mater. Sci. Eng.* **10** 437–468.